

*KRZYSZTOF LIPIŃSKI \**

## RIGID FINITE ELEMENTS AND MULTIBODY MODELLING USED IN ESTIMATION AND REDUCTION OF ROD VIBRATIONS

In the paper, a mechanical set composed of a robot (manipulator) and of an elastic beam is considered. The beam is fixed to the top of the robot structure. In most of similar cases, undesired vibrations can be excited in the beam. They create an especially significant problem when dynamics in the robot braking period is examined. In the paper, estimation and modification of length of the braking period is proposed, in order to reduce the undesired vibrations. Investigations are restricted to numerical models, only. The rigid finite elements modelling and the multibody modelling are used together to obtain the numerical model required for the system. Instead of the classical rigid finite elements, its modified version is used, where some of the relative deformations are locked between the neighbour elements. As a result, sizes of the obtained matrices can be reduced as well as the time of the numerical calculations.

### 1. Introduction

In the paper, dynamics of some mechanically non-homogenous sets is under consideration. In the sets, a beam is moved by an actuated robot. Concerning the robot, its structure is composed of rigid links, while the beam is considered as elastic and long. Displacements at the robot joints are considered as significant, while the beam deformations are relatively small. The beam is fixed to the terminal point of the robot structure (e.g., the flexible element rigidly gripped, placed in the gripper; the gripper is located on the end of the last element of mechanical structure of the robot). Finally, some significant displacements are necessary to move the beam to its destined position. In spite of the introduced non-homogeneity, a common model is prepared for the considered system.

---

\* *Gdansk University of Technology, Faculty of Mechanical Engineering, ul. Narutowicza 11/12, 80-233 Gdansk, Poland; E-mail: klipinski@pg.gda.pl*

Operating with an element fixed to the robot gripper may not be treated as a straightforward problem, in particular when significant motions are necessary, and when the operated beams are long and elastic. Additional considerations are necessary when the movement should be performed properly. Few methods can be applied to operate the robot equipped with the long elastic element.

First, when a single robot is used, a set of disadvantages must be accepted. For example, significant torques can be present in fragile places of the robot structure (sourced in the gravitational effects of the beam). Especially endangered are the gripper structure and the structure of the wrist joints, as well. The torques are especially critical, when the robot/beam fixing point is far from its potentially optimal position (e.g., it is far from the centre of the gravity force of the beam). The beam's significant inertia has to be considered, also. It reduces the wrist acceleration possibilities, and significant wrist torques are necessary to accelerate such rotations. High angular precision in the wrist positioning is necessary, when high precision of the beam terminal point positioning is required. Finally, (but in some cases it is the most fundamentally, also) significant beam vibrations can easily be excited. The excited vibrations can be difficult to eliminate, their duration can be long. Often, the excited vibrations can persist up to the period when the robot operation is finished (i.e., to the period when the destined position is obtained by the robot and the driven links are stopped). Unstable and chaotic behaviours can be observed, when frequencies and amplitudes of the imposed excitations are set in some critical ranges for the beam [1, 2].

In-between the alternative operation methods, operations on a set of robots can be pointed as useful, especially in the cases when long and elastic beams are moved. Some ideas related to it were discussed in [3, 4], where fruitfulness of the idea is pointed. However, disadvantages are associated with this method, too. For example, significant internal forces and torques (and beam stresses, as well) can be observed in the sections of the beam. These stresses can be non-required, especially when plastic and fragile elements are moved. To eliminate them, sophisticated collaboration of robots is necessary. However, low cost robots are considered in the presented case (potential price of the carried element is low), therefore expensive and sophisticated robots are economically unjustified in the task. It reduces the necessary collaboration possibilities, as information exchange is impossible or limited between the planned control units.

The following evident and attractive alternative can be considered. It is concerned with active, semi-active or passive damping elements. Installation of such elements can solve the vibrations problem and help us to control the ranges of the undesired vibrations. However, the method should be re-

jected from the economical reasons, again. The necessary installation and des-installation of the damping elements (required respectively for each of the moved objects) can be time and cost consuming problem.

In the present paper, a subsequent alternative is proposed. Presuming the beam vibration as significant, easy for excitation and difficult for damping, sophisticated driving strategy is sought after for the robot. The strategy must reduce the beam vibrations, especially in the post operation period. Two options are possible. In the first one, the robot structure is used as the active damping structure, and its control unit (i.e., the control unit of the robot itself) is used as the control unit of the damping structure, as well. As the alternative option, operations with length of the braking time can be proposed. In these cases, length of the braking period must be well synchronised with periods of the beam vibrations. Potential effects of the proposed correlations are investigated and presented in the paper.

In the paper, modelling, control and dynamics of a continuous sub-system (an elastic beam) is a significant aspect of the considerations. To deal with dynamics of the beam, a technique of rigid finite elements (*RFE technique*) [5, 6, 7, 8] is employed. Focusing on the most critical ideas, used in the background of the proposed discretization algorithm, we refer to the ideas introduced initially by Kruszewski et al. [5]. Separations in space are performed on the physical properties of the beam, in a dedicated manner. As a result, inertia and elasticity parameters are separated and concentrated in some geometrically distant places. As the main benefit, the obtained model is relatively simply and effective. Although several decades have passed, and computer science revolution recently takes place, the *RFE technique* remains vital and attractive. It was used intensively over last decades and it is used intensively by the present-day researchers, too. A significant number of researchers have investigated its details and they have modified the method to increase its flexibility and applicability, as well. It resulted in numerous modifications and the initial version proposed by Kruszewski is treated as a classical reference algorithm at present. The classical and the modified method were described extensively, and a number of related works can be recalled (e.g. [6, 7, 8]).

In accordance with the presumption of the presence of a significant drift motion, the rigid finite elements modelling (*RFE modelling*) and the multi-body system modelling (*MbS modelling*) [9, 10, 11, 12] are joined to compose the common model. Thanks to this action, benefits of the two modelling methods can be used more effectively. Moreover, to reduce the sizes of the calculated matrices, *modified rigid finite elements method* [8] is used, instead of the classical one described in [5, 6]. In the modified version, some of the lower order relative deformations are constrained, considered as negligible

and locked. Instead of the additional constraint equations, kinematic chain structures are defined. As a subsequent consequence, the joint coordinates are used as the system generalised coordinates (instead of the absolute coordinates used in the classical *RFE* modelling method). Then, one of the classical *MbS* modelling methods is used to obtain dynamics equations of the proposed kinematical chain. The engaged modelling method is based on relations present in the kinematical chains. They are used to determinate kinematics and dynamics equations: to estimate velocities and accelerations of the bodies of the system (kinematics); to express dynamics of the free body diagrams (the Newton/Euler dynamic equations); to eliminate the unknown joint interactions present in the joint locked directions (the kinetostatic principle); to obtain the scalar form of the searched dynamic equations (projections of the joint torques and forces). As a result, a mixed numerical algorithm is constituted. It is based on a simultaneous use of the introduced multibody rules, both for the robot mechanical links and for the beam chains of rigid finite elements, as well.

The paper is divided into six sections. The subsequent one (i.e., the one after the introduction) presents the main assumptions used to prepare the rigid finite element physical model of an elastic beam. In the third section, backgrounds of the used multibody equations are presented. In the fourth section, numerical tests are presented. The tests presented in this section are restricted to planar cases, only. The beam and the robot are modelled as planar multibody systems. Different lengths of the braking periods, as well as different damping properties, are tested for the model. In the fifth section, a spatial model is analysed. As in the previous one, different lengths of the braking periods are tested. Their influences on the beam deformations are analysed for different directions of the deformations. The final sixth section is devoted to presenting some summary and the conclusions.

## 2. Background of the used rigid finite element modelling method

In this paper, dynamics of a continuous sub-system (an elastic beam) is considered. To deal with its dynamics, rigid finite element technique is employed for discretization. The engaged discretization technique refers to a technique proposed by Kruszewski et al. [5]. To consider the beam significant drift motion, and to reduce the sizes of the calculated matrices as well, the *modified rigid finite elements method* [8] is used, instead of the classical one described in [5, 6].

As in the original method proposed by Kruszewski et al. [5], to obtain the discrete model of the considered cylindrical beam, four steps are performed: the beam is divided into sections and a set of  $m$  sections (of equal lengths



$\Delta$ ) is obtained; flexibility and damping features are concentrated as a point flexibility and placed in the centres of these sections (it constitutes *elasto-damping elements (SDE)* responsible for beam deformation) (Fig. 1a); the remaining parts of the segment are stiffened (are supposed to be filled by a rigid and material substance); the adjoining sub-segments are joined, with a restriction that the joined sub-segments must not be separated by any of the *SDEs* present in the system (it constitutes *rigid finite elements (RFE)* responsible for the beam inertia) (Fig. 1a). Concerning to their masses, shapes and their inertia moments, the introduced *RFE* should coincide with the original parts of the initial beam. According to the same idea, the *SDE* elasto-damping properties should be selected in accordance to the initial beam elasto-damping properties. More of the necessary presumptions, descriptions and details, as well as the related formulas can be found in [5, 6, 7, 8].

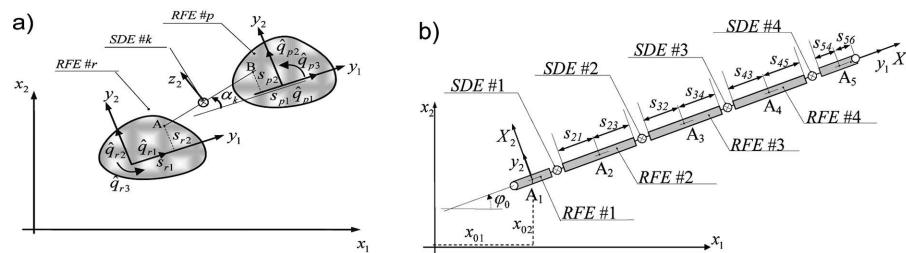


Fig. 1. Considered elements: the *RFE*'s coordinates (a); the beam classical discretization (b)

In the presently considered cases, there are some of the tests conditions (i.e., the beam motion especially) which are slightly broadened in comparison to the initial cases proposed by Kruszewski et al. [5]. Two of the properties have to be pointed out: significant drift motion must be considered at the same time when small relatively deformations (the *SDEs* deformations) are considered in the beam (the possible simplification resulting from the negligible values are applicable in the model); next, the system linearity (announced in [5]) may not be preserved, and more detailed nonlinear models should be prepared for the system (significant effects of the introduced drift motion).

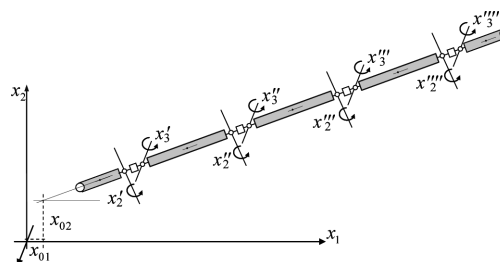


Fig. 2. Modified formulation of the rigid finite elements discretization

To solve the introduced problems, a modified formulation is used instead of the classical one. Main concepts proposed by Wojciech [8] are recalled. Four ideas are fundamental in the modification: a concept of a kinematical chain (see Fig. 2) is introduced (the concept is introduced to replace the initial system, where a set of independent bodies is introduced and then connections via a set of the springs-dampers elements are added); a concept of a multi degree-of-freedom joints is introduced (they are engaged to replace the six degrees of freedom *SDEs* used in the classical formulation); the joint coordinates are used as the system generalized coordinates (in opposition to *RFE* absolute coordinates used in the initial method proposed by Kruszewski et al. [5]); not all of the relative displacements are allowed in the introduced joints (e.g., the observed effects of relative translational deformations are insignificant in comparison with bending deformations and their effects as well). Thanks to the modifications, a set of beneficial features can be observed in the modified model (e.g., sizes of the system matrices, as well as the number of mathematical calculations are lower).

A significant difference, in comparison with the method proposed by Wittbrodt et al. [7], must be underlined, however. Homogenous transformations, as well as Denavit-Hartenberg coordinates will not be employed in the present paper. Alternative version of multibody modelling is recalled. In the past, a number of tests were performed to valid efficiency of the proposed modified version. The tests and details of the employed method were presented in some of the earlier papers, e.g., ([13, 14, 15]).

### 3. Background of the used multibody modelling method

The paper used presumptions, as well as the main equations, of the proposed multibody modelling that are recalled from [9, 10, 11, 12]. In accordance to the recalled paper, the considered multibody system (*MbS*) is assumed as a set composed of non-deformable, inertial *rigid bodies* (Fig. 3a). Besides of the whole-system-motions, relative displacements are possible, too (the analysed bodies can change their relative position and orientations), and the potential changes are considered as significant. The relative motions may not be treated as free, six-degrees-of-freedom motions. Some restrictions are present (some directions are locked for the relative motions). According to it, a useful concept of *connections* is introduced to describe deformations the system, and the *neighbour body* is proposed as the name for any of the generic couples of bodies interconnected with use of the announced generic connection. Connections are massless. They concentrate on deformability, propulsion, damping and elasticity features, only.

In general, the introduced connections can be defined as multi degrees-of-freedom elements. However, as it was pointed out in a number of related works (e.g., [9, 10, 11, 12]), one-degree-of-freedom elements of prismatic or revolute type are sufficient to describe any of the connections (and any of the potential *MbS*, too) since each of the multi-degrees-of-freedom connections can be modelled as an ordered sequence of the one-degree-of-freedom connections, massless bodies and constraints when necessary. Such a restricted, one-degree-of-freedom connections are called the *joints* (Fig. 3a), in general. Finally, the term *kinematical chain* (*kCh*) (Fig. 3a) is proposed to refer to each of the sequences of bodies connected by joints, and (without engaging in the discussion about the potential benefits and the potential drawbacks), the relative joint displacements (*joint coordinates*) are considered as the *system coordinates* (*SC*) [9, 10, 11, 12, 16].

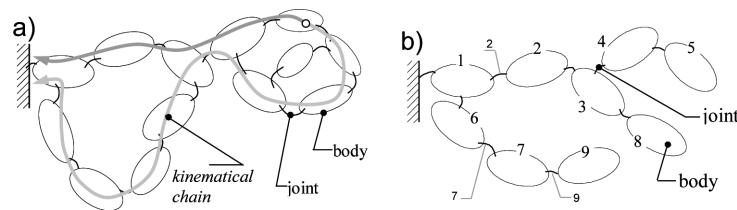


Fig. 3. Exemplary multibody systems: closed kinematical chains (a); a tree structure and its numbering proposition (b)

In the used description, the most fundamental concept is the *reference kCh*, i.e., it is the *kCh* between the considered  $B^i$  and the motionless *reference body*  $B^0$  (denoted as  ${}^0kCh^i$  in this paper). When the contents of the  ${}^0kCh^i$  are determined in a unique way, the *chain* is understood as *open*. Otherwise, a *closed kCh* is present in the system structure (Fig. 3a). The last ones (i.e., the closed *kCh*) will not be considered in the present paper. As a tree structure is considered, a *body numbering* can be introduced (Fig. 3b). The numbering is correlated directly with the succession order, i.e., when a generic body  $B^j$  belongs to  ${}^0kCh^i$ , then its number is lower, or at least it is equal, to  $i$ . According to the numbering rule, a modified symbol of relation is introduced. At the context of the system topology, the  $j < i$  symbol implies that the announced  $B^j$  element must belong to the reference chain of the announced  $B^i$  element (to the  ${}^0kCh^i$ ). Moreover, to deal with the complete set of  $B^i$  *direct successors*,  $i^+$  symbol is introduced. Finally, the joint between the  $B^i$  and its direct predecessor is numbered as  $i$  and denoted as  $J^i$  for simplicity.

## KINEMATICS AND DYNAMICS OF THE TREE STRUCTURES

Let us consider a generic vector  $\vec{a}$  fixed to the generic body  $B^i$ . As the system-considered bodies are rigid, the vector coordinates are constant when evaluated in the body fixed frame. Orientation matrices,  $\mathbf{T}^i$ , are necessary to express them in the motionless frame, fixed to the system reference body. A similar conclusion can be proposed when vectors of the absolute position of the body mass centre,  $\vec{x}^i$ , measured with respect to the origin of the fixed frame, are analysed.

In the so-called assembling configuration [11] (defined by zero displacement set for the  $SC$ ), co-linearity of the frames is proposed for all the frames fixed to the system bodies. Then, referring to symbols presented in Fig. 4, ones can write the following formulas [9, 10, 11, 12]:

$$\mathbf{T}^i = \prod_{j:j \leq i} \mathbf{R}^j; \quad \vec{x}^i = \sum_{j:j \leq i} (\vec{z}^j + \vec{a}^{ji}) = \sum_{j:j \leq i} \vec{l}^{ji}; \quad (1ab)$$

$$\vec{\omega}^i = \sum_{k:k \leq i} \dot{\varphi}^k \cdot \vec{e}^k; \quad \dot{\vec{x}}^i = \sum_{k:k \leq i} (\dot{p}^k \cdot \vec{a}^k + \vec{\omega}^k \times \vec{l}^{ki}); \quad (2ab)$$

$$\dot{\vec{\omega}}^i = \sum_{k:k \leq i} (\ddot{\varphi}^k \cdot \vec{e}^k + \dot{\varphi}^k \cdot \vec{\omega}^k \times \vec{e}^k); \quad (2c)$$

$$\dot{\dot{\vec{x}}}^i = \sum_{k:k \leq i} (\ddot{p}^k \cdot \vec{a}^k + \dot{\vec{\omega}}^k \times \vec{l}^{ki} + 2\dot{p}^k \cdot \vec{\omega}^k \times \vec{a}^k + \vec{\omega}^k \times (\vec{\omega}^k \times \vec{l}^{ki})), \quad (2d)$$

where:  $\mathbf{R}^j$  – relative orientation matrix that expresses orientation change present in the  $J^i$  joint;  $\vec{a}^j$  – unit vector collinear to the translation line (it is a nonzero vector for the translational joints and zero vector when rotational joint is considered);  $\vec{e}^j$  – unit vector collinear to the rotation axis (it is a zero vector when translational joint is considered).

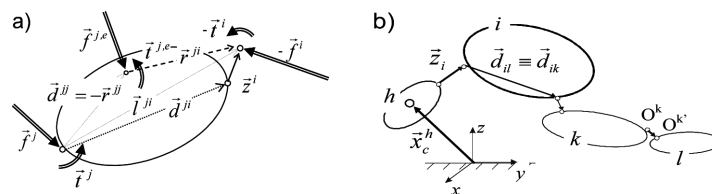


Fig. 4. Elements of the considered multibody system: geometrical dimensions of  $B^j$  and interactions acting on the body (a); multivariational description of  $B^i$  dimensions used in the multibody system (b)

According to the idea detailed in [11], when some tables of vectors are introduced, Eqs. (2) can be written in some matrix-like form [10, 11]:

$$\vec{\omega}^i = \vec{\mathbf{A}}^{2,i} \cdot \dot{\mathbf{q}}; \quad \dot{\vec{x}}^i = \vec{\mathbf{A}}^{1,i} \cdot \dot{\mathbf{q}}; \quad \dot{\vec{\omega}}^i = \vec{\mathbf{A}}^{2,i} \cdot \dot{\mathbf{q}} + \vec{\omega}^{i,R}; \quad \dot{\dot{\vec{x}}}^i = \vec{\mathbf{A}}^{1,i} \cdot \dot{\mathbf{q}} + \dot{\vec{x}}^{i,R}, \quad (3a-d)$$





where:  $\mathbf{q}$  – column matrix of  $SC$ ;  $\vec{\mathbf{A}}^{1,i}$ ,  $\vec{\mathbf{A}}^{2,i}$  – row tables with vectors as their element;  $\vec{x}^{i,R}$ ,  $\vec{\omega}^{i,R}$  – acceleration “remainders”, independent to joint accelerations.

To obtain the *dynamic equations (DE)*, the connecting points between all the  $B^i$  and the  $J^i$  are cut and replaced by the joint interactions (Fig. 4a). Free body diagrams are composed for the bodies and the Newton/Euler dynamics equations are used [9, 10, 11, 12]:

$$m^i \cdot \ddot{x}^i = \vec{f}_i + \vec{f}_i^e - \sum_{j \in i^+} \vec{f}_j^i; \quad (4a)$$

$$\vec{\omega}^i \times (\vec{I}^i \cdot \vec{\omega}^i) + \vec{I}^i \cdot \dot{\vec{\omega}}^i = \vec{t}_{iC} + \vec{r}^{ii} \times \vec{f}_i + \vec{t}_{iC}^e - \sum_{j \in i^+} \vec{t}_{jC}^i - \sum_{j \in i^+} \vec{r}^{ij} \times \vec{f}_j^i, \quad (4b)$$

where:  $m^i$  – mass of  $B^i$ ;  $\vec{I}^i$  – its tensor of moments of inertia calculated about the  $B^i$  mass centre;  $\vec{f}^i$ ,  $\vec{t}^i$  – force and torque at the  $B^i/J^i$  cutting point;  $\vec{f}_i^e$  – net external force supposed as acting at mass centre of  $B^i$ ;  $\vec{t}_{iC}^e$  – net external torque acting at the  $B^i$  (calculated about its mass centre).

Next, the *DEs* (4) are combined with the velocity and acceleration Eq. (3).

Moreover, to eliminate the successor forces and torques from Eq. (4), kinetostatic principle is used as described in [11] According to this rearrangement, the searched  $J^i$  interactions can be written as [11]:

$$\vec{f}^i = \vec{\mathbf{C}}^{1,i} \cdot \ddot{\mathbf{q}} + \vec{\mathbf{D}}^{1,i} + \vec{\mathbf{E}}^{1,i}; \quad \vec{t}^i = \vec{\mathbf{C}}^{2,i} \cdot \ddot{\mathbf{q}} + \vec{\mathbf{D}}^{2,i} + \vec{\mathbf{E}}^{2,i} \quad (5)$$

Finally, when interactions from (5a) are projected onto joint mobility vectors (for translational joint, they are projected on the  $\vec{a}^i$  vectors and for rotational joint on the  $\vec{e}^i$  vectors respectively), and when components are stored in corresponding matrices, the system *DE* can be expressed as [9, 10, 11, 12]

$$\mathbf{M}(\mathbf{q}) \cdot \ddot{\mathbf{q}} + \mathbf{F}(\dot{\mathbf{q}}, \mathbf{q}, \mathbf{f}_e, \mathbf{t}_e, t) = \mathbf{Q}, \quad (6)$$

where:  $\mathbf{M}$  – mass matrix;  $\mathbf{F}$  – column matrix composed of velocity depend inertial effects;  $\mathbf{Q}$  – column matrix composed of joint actuations;  $\mathbf{f}_e$  – column matrix composed of the external forces acting on the system bodies;  $\mathbf{t}_e$  – column matrix composed of the external torques acting on the system bodies;  $t$  – time.

#### 4. A planar system and the numerical tests related to it

To visualise the potential benefits in the proposed method (vibration ranges are reduced by operating with the length of the braking period), two numerical models are proposed in the paper. The first one is based on a



planar object. A RRR planar robot with a relatively long and flexible final link is analysed. The physical model of the object is visualised in Fig. 6. Its final link is considered as the only flexible element in the model. Length of the first arm (#1 in Fig. 6a) equals 0.2 m, and its mass is estimated to 0.63 kg. Its inertia moment (about the mass centre) is 0.00061 kg·m<sup>2</sup>. Its mass centre coincides with the geometrical centre of its length. For the second arm (#2 in Fig. 6a), its length equals 0.3 m, and its mass is estimated as 0.95 kg. Its inertia moment (about the mass centre) is 0.001781 kg·m<sup>2</sup>. Again, its mass centre coincides with the geometrical centre of its length. The final, flexible link is 1 m long and it is considered as a steel, cylindrical beam of 0.02 m diameter, constant along all length of the link.

#### PHYSICAL MODEL OF THE CONSIDERED STRUCTURES

To discretize the flexible link, the *RFE* discretization is employed. In the initial step, a set of ten segments is selected (all being identical in lengths). Their elastic properties are concentrated in geometrical centres of the segments. As a result, a set of ten identical *SDE*s is introduced in the model. After adjoining of the neighbour sub-segments, a set of nine identical *RFE*s is obtained, completed with two outermost *RFE*s considered as the twice shorter ones. Lengths of the nine central elements equal 0.1 m. Their masses equal 0.315 kg and their inertia moments are 0.0002625 kg·m<sup>2</sup>. For the shorter elements, it is 0.05 m, 0.1575 kg and 3.28125·10<sup>-5</sup> kg·m<sup>2</sup>, respectively. Mass centres (for the standard and the shorter *RFE*) coincide with their geometrical centres. According to the method proposed in [8], all the introduced *SDE*s are considered as single degree of freedom relative joints, restricted to rotational degrees of freedom, only. The elasticity coefficient (associated with rotational deformations at this relative revolute joint) equals 1.5865·10<sup>4</sup> N·m/rad, and its damping coefficient is varying from 1 to 5 N·m·s/rad depending on the test.

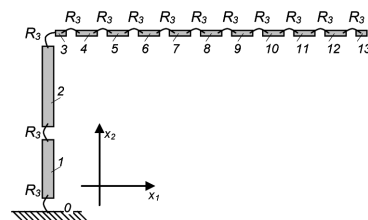


Fig. 5. Multibody model of the considered planar system

With some classical blocs and symbols as these used in [9, 10, 11, 12], a sketch of the resulting structure (which combines the primary robot model

with the *RFE* model of the flexible link) is presented in Fig. 5. The structure is modelled as a typical *MBS* next.

## NUMERICAL TESTS

For initial configuration of the tests, the system takes it vertically/horizontally position. The corresponding sketch is presented in Fig. 6a. The first and the second arm (robot) are placed vertically and the third one (the elastic beam) is positioned horizontally. Next, all the revolute joints of the robot structure (the initial-three joints of the multibody structure) are considered as driven. Their velocities are time dependent. In the initial period of motion, constant velocities are considered for all the driven joints of the system (joints #1, #2 and #3, as presented in Fig. 6a). In all the tests, the introduced initial velocities equal  $\pi/4$  rad/s;  $\pi/4$  rad/s and  $\pi/2$  rad/s for joints #1, #2 and #3, respectively. Next, in the sub-subsequent period of motion, constant decelerations are considered in the driven joints. The used deceleration values depend on the test illustrative parameter (they are calculated individually for each of the considered tests).

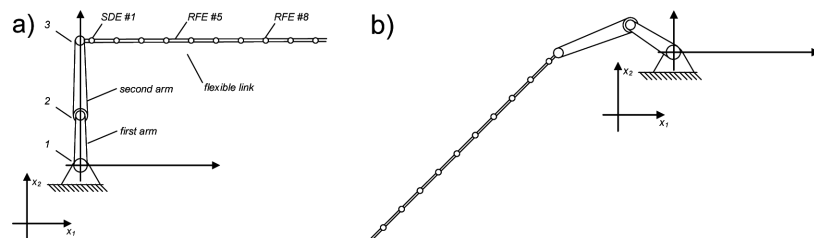


Fig. 6. Sketches of the considered planar robot: initial position (a); final position (b)

The considered tests should illustrate relations between the lengths of the braking period,  $\Delta t_b$ , and the dynamic behaviour of the driven beam. When corresponding decelerations at the driven joints are evaluated, they have to be precisely adjusted to the initial velocity values and to the length of the braking period (Fig. 7). They must ensure that the stop of the joint motions will appear in the imposed braking time. Moreover, assuming the initial and final positions of the robot are preserved for all the tests of this series, the time of the beginning of the braking period,  $t_{bo}$ , should depend on the test illustrative parameter, too (it has to be fitted to the presumed length of the braking period). Let us underline, in addition, the final instant of motion is not preserved in the tests.

The final instant of the braking period,  $t_{bf}$ , (i.e. the stop of the robot) does not indicate the end of the simulation. The subsequent period of the simulation illustrates evolutions of the beam excited vibrations. In this period, the beam vibrations are the primary of the observed parameters.

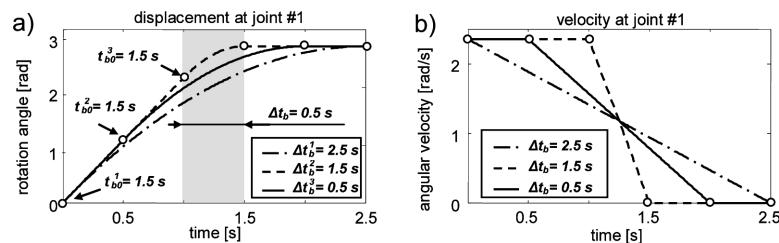


Fig. 7. Some examples of joint breaking characteristics: displacement (a); velocity (b)

To avoid the presence of significant vibrations potentially observed in the initial period of motion (the constant speed motion), the initial equilibrium position is sought-after for all the displacements present in the *SDEs* used to model the elastic link of the robot (with the imposed, non-zero velocities of motion of the initial joints of the robot).

To visualise the sought-after property, three series of tests are performed. In the first series, relatively high damping properties are considered. Identical damping of  $c_i = 5 \text{ N}\cdot\text{m}\cdot\text{s}/\text{rad}$  is set for all the *SDEs* used to model the flexible link (i.e., the final link of the system). Two different lengths of the braking periods are considered in this series. The first period is  $0.507 \text{ s}$  long, while the second is considered as slightly ( $8.1\%$ ) shorter, (i.e., its duration takes  $0.466 \text{ s}$ , only). Joint deformations are observed at the fourth joint of the considered *MBS* structure (i.e., the joint used to model first *SDE* of the elastic link) (see Fig 6a). The obtained deformations are presented in Fig. 8.

As it can be expected, the announced three sub-periods of motion are easy to observe in the characteristics (Fig. 8a). The first, denoted as **A** in the figure, corresponds to the initial sub-period characterised by the constant values of the joint velocities. The second, denoted as **B**, is associated with the braking sub-period. It can be seen in the figure, without any difficulty, that according to the suddenly introduced decelerations, the beam modifies its equilibrium position (deformed with respect to the previous one) rapidly. Moreover, the beam position valid in the previous step of the simulation is far from the new equilibrium. It can be treated as a kind of the beam initial deflection, and significant vibration can be observed about the new equilibrium, next. The final sub-period, denoted as **C** in the figure, corresponds to the period when the stopped robot is considered. Again, the decelerations change rapidly at the beginning of this sub-period (they disappear rapidly) and the beam equilibrium position re-configure rapidly, too. According to the beam initial deflection (i.e., its initial position observed at the beginning of the period **C**), the observed ranges of vibrations can vary significantly in final sub-period of the simulation (Fig. 8a versus Fig. 8b).

The observed results have confirmed that the range of the beam vibrations can be reduced significantly, when the time instant related to the end of the

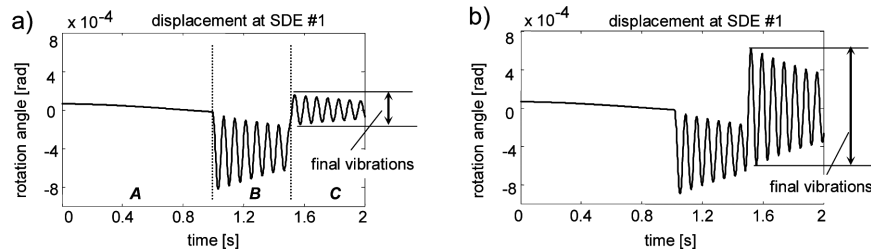


Fig. 8. Displacements at the selected *SDEs* of the modelled flexible beam (upper value of damping): longer period of braking (a); shorter period of braking (b)

braking period is adjusted precisely with the beam vibration characteristic. The undesirable vibrations can be eliminated or at least reduced at the considered sub-period *C*. The initial hypothesis is verified positively in the test. As it is shown in the results (Fig. 8a versus Fig. 8b), the modification of the length of the braking period can lead to a set of some potentially fruitful effects.

To verify the effectiveness of the proposed concept, additional series of tests are performed. Lower value of damping is considered, i.e., damping of  $c_i = 1 \text{ N}\cdot\text{m}\cdot\text{s}/\text{rad}$  is set to all the *SDEs* used to model the final link of the system. Again, two different lengths of the braking periods are considered. The first period is slightly longer (in comparison with the one used in the initial series of the tests). It is set to  $0.509 \text{ s}$  long (it is modified mainly as the vibration frequency depends slightly on the used damping coefficient). The length of the second period is set to  $0.469 \text{ s}$ , only. Again, joint deformations are observed at the first *SDE* (see Fig 6a). The obtained results are presented in Fig. 9.

Again, the results confirm the benefits associated with the correlations between the beam vibration characteristic and the length of the braking period. When correlated optimally, vibrations can be reduced significantly (especially in the final sub-period *C*, when the driven joints are stopped). Moreover, the obtained results (Fig. 9) have indicated clearly that the presently considered case (lower damping coefficients) is notably better in compare to the case considered previously.

To obtain some alternative zoom on the obtained effects, an additional series of calculations is performed. The motion of the beam farthest point is observed, and its vertical position is calculated. The obtained characteristics are presented in Fig. 10, where a comparison is presented between the results obtained for different lengths of the braking periods. The zoom is focused on the final vibrations, only. To facilitate the comparison, identical scale is used in the two neighbour sub-plots. The vibrations obtained for the longer period of braking (range of these vibrations is about  $0.12 \text{ mm}$  high), seen

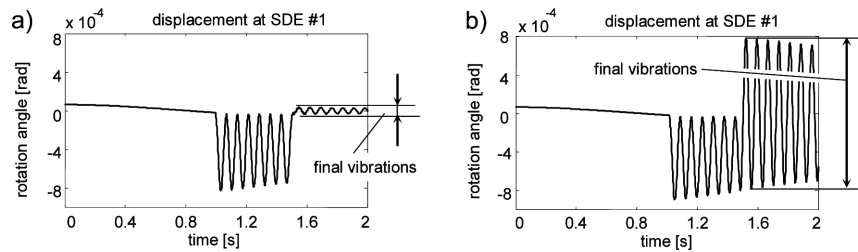


Fig. 9. Displacements at the selected *SDEs* of the modelled flexible beam (lower value of damping): longer period of braking (a); shorter period of braking (b)

in Fig. 10a, are compared with 25 times greater (their range is about 3 mm) vibrations obtained for the shorter period, shown in Fig. 10b.

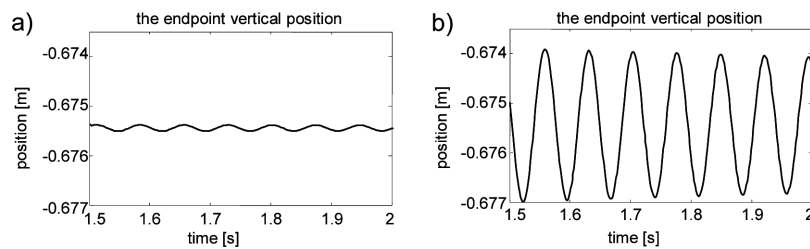


Fig. 10. Vertical position of the terminal point of the final link of the robot (final period of simulation and lower value of damping): longer period of braking (a); shorter period of braking (b)

### 5. A spatial system and the numerical tests related to it

In the subsequent series of tests, a spatial case is considered, i.e., some more challenging case is considered compared to the previously considered planar one. A physical model of the system is depicted in Fig. 11. The final link of the robot (denoted as #5 in Fig. 11a) is considered as an elastic beam. Its length is significant and its cross section is relatively small. For the rest of the links, they are considered as rigid ones. The initial element of the considered robot (i.e., the base closest element, denoted as #1 in Fig. 11a) refers to the rotating column of the robot. The column is 0.7 m high, and its mass is estimated as 35 kg. Its inertia moments (about the mass centre) are 1.5412 and 0.224 kg·m<sup>2</sup> respectively for perpendicular and lengthwise directions. Its mass centre coincides with the geometrical centre of its height. For the first arm (element #2 in Fig. 11a), its length equals 1.5 m, and its mass is estimated as 20 kg. Its inertia moments are (again, about the mass centre) 3.766 and 0.032 kg·m<sup>2</sup>, respectively, for perpendicular and lengthwise directions. Its mass centre coincides with the geometrical centre of its length. The second arm (element #3 in Fig. 11a) is identical to the first arm. The

wrist (combined with the initial *RFE* of the discretized link) is  $0.08$  m long, for the distance measured in the direction of the  $y$  axis. Its mass equals  $0.5$  kg and its inertial moments are  $0.00026667$  and  $0.00013333$   $\text{kg}\cdot\text{m}^2$ , respectively. The final, flexible link is  $2$  m long and the link is considered as homogenous, cylindrical beam made of steel. Its diameter is  $0.02$  m and it is presumed as constant along whole the length of the beam.

### PHYSICAL MODEL OF THE CONSIDERED STRUCTURES

To discretize the flexible link, the *RFE* modelling method is employed, again. In the initial step of the discretization, a set of nine segments is selected. Their lengths are equal. The elements elastic properties are concentrated in their geometrical centres. As a result, a set of eight identical *SDEs* is introduced into the model. With/after adjoining the neighbour sub-segments, a set of eight identical *RFEs* is obtained, completed with two outermost considered as the twice shortened ones. The initial *RFE* (the one being the closest to the robot structure) is joined rigidly with the gripper and it appears in the model indirectly, as an augmented mass and inertia of the gripper. Concerning the rest of the elements, lengths of the main elements equal  $0.2$  m. Their masses equal  $0.49071$  kg and their inertia moments are  $0.0016357$   $\text{kg}\cdot\text{m}^2$  and  $2.45355\cdot 10^5$   $\text{kg}\cdot\text{m}^2$  for the perpendicular and the lengthwise directions, respectively. For the final element, its reduction (as well as reduction of all of its physical parameters) to the twice shortened length is considered. Mass centres (for the standard and the shortened elements) coincide with their geometrical centres.

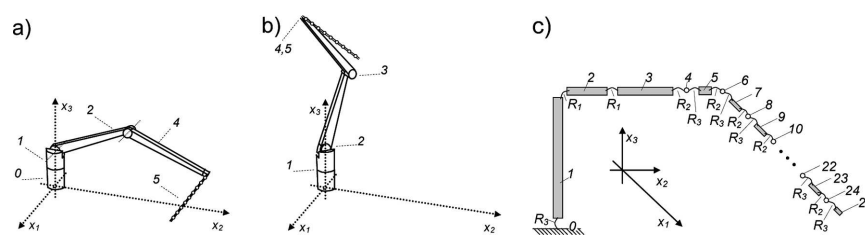


Fig. 11. Spatial robot: its initial position (a); its final position (b); its multibody model (c)

According to the idea proposed in [8], the introduced *SDEs* are considered as elastic universal (Cardan) linkages placed between the neighbouring *RFEs*. The bending elasticity coefficients are considered, only. In the next step, the Cardan linkages are modelled as composed structures. They are built of two rotational joints interconnected by a fictitious massless-dimensionless body (Fig. 11c). Their axes of rotations are perpendicular one to the other, and they are perpendicular to the lengthwise axis of the beam, too (Fig. 2). All the elasticity coefficients (associated to rotational displacements at the in-

roduced *SDEs* joints) are coherent with the bending properties of the driven beam. They are equal to  $7.93252 \cdot 10^3$  N·m/rad. Related damping coefficients are set to 10 N·m·s/rad.

Again, with the use of classical blocs and symbols presented in [9, 10, 11, 12], a sketch of the resulting structure (which combines the primary robot model with the *RFE* model of the flexible link) is presented in Fig. 5. As some significant displacements are present in the system, the structure is modelled as a typical *MbS*, next.

## NUMERICAL TESTS

For the tests initial configuration, its sketch is presented in Fig. 11a. The column (body #1) is set vertical and it can rotate about the vertical axis,  $x_3$ . The rest of the links (arms #2 and #3) is placed in  $x_2$ - $x_3$  plane. The link #2 is tuned up about  $\pi/4$  rad, while the link #3 is turned down about the same angle. Both the rotation axes of the links are collinear with  $x_1$  axis in the system (when they are at the system initial position). The beam takes it horizontal position (collinear with  $x_1$  axis in the system, too). Next, all the revolute joints of the robot structure (the initial-three joints of the multibody structure) are considered as driven. Their velocities are time dependent, as the simulation period is divided into three structurally different sub-periods. In the initial period of motion, constant velocities are considered for all the driven joints of the system (joints #1, #2 and #3, as presented in Fig. 11b). In all the tests, the introduced initial velocities equal  $\pi/4$  rad/s;  $\pi/4$  rad/s and  $\pi/2$  rad/s for joints #1, #2 and #3, respectively. Joints #4 and #5 (the wrist of the gripper) are locked on permanent zero value. Next, in the sub-sequent period of motion, constant decelerations are considered in the driven joints. The used deceleration values depend on the test illustrative parameter (they are calculated individually for each of the considered tests).

Again, lengths of the braking period,  $\Delta t_b$ , are taken as the test illustrative parameter. According to it, all the decelerations present in the robot driven joints have to be precisely adjusted to the initial values of the joint velocities and to the length of the braking period (Fig. 7). Similarly as in the tests presented in the previous section, the complete length of the motion period is not a preserved parameter. It varies between the tests. Assuming that the initial and final positions of the robot are preserved for all the tests of this series, the time of the beginning of the braking period,  $t_{bo}$ , must be correlated with the test illustrative parameter (it should be fitted for the presumed length of the braking period). According to the same reasons, the final instant of motion is the test depending parameter, too.



As in the planar case, the final instant of the braking period,  $t_{bf}$ , does not indicate the end of the simulation. The subsequent period of the simulation illustrates evolutions of the beam excited vibrations. In this period, the beam vibrations are the primary of the observed parameters.

To avoid the presence of the significant vibrations potentially observed in the initial period of motion (the constant speed motion), initial equilibrium position is sought-after for all the displacements present in the *SDEs* used to model the elastic beam (with the imposed, non-zero velocities of motion of the initial joints of the robot).

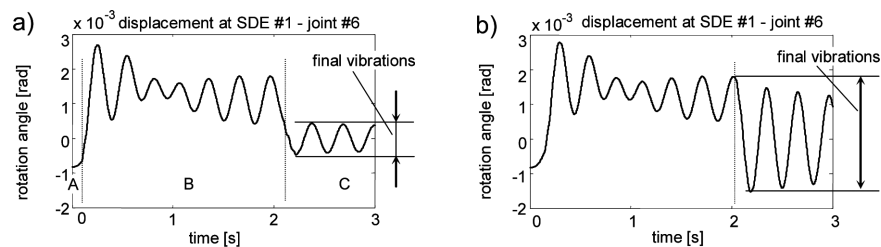


Fig. 12. Displacements at selected *SDEs* of the modelled flexible beam (first direction of bending): 2s braking period (a); 1.9s braking period (b)

To visualise the investigated property, a series of tests is performed. Two different lengths of the braking periods are considered in this series. The first period is 0.2 s long, while the second one is considered as slightly shorter, (i.e., its duration takes 1.9 s, only). Joint deformations are observed at sixth and seventh joint of the considered *MBS* structure (i.e., at the joints used to model the first *SDE* of the elastic beam) (see Fig. 11c). The obtained results (for different directions of the *SDE* deformations) are presented in Fig. 12a and Fig. 13a.

The three crucial periods of motion (announced previously) are easy to observe in Fig. 12a. Again, similar mechanism of vibrations can be observed in the test. The equilibrium position of the braking period (deformed with respect to the equilibrium of the constant velocity motion) arises rapidly according to the suddenly introduced decelerations, and the beam starts to vibrate significantly around the new deformed equilibrium position. The situation changes again at the simulation final sub-period *C*. Joint decelerations are re-changed rapidly again (they disappear rapidly) and the beam equilibrium position re-changes rapidly, too. As a result, a new set of vibrations is excited about the new equilibrium position.

Again, according to the remarks made in the previous section, it is vital to point out that the range of the beam vibrations can be reduced significantly, when the length of the braking period is adjusted precisely with the beam dynamics properties. Some of the undesired vibrations can be eliminated or

at least reduced at the considered sub-period *C*. This hypothesis, verified previously in the planar case, is verified positively in the present case, too. As it is shown in the results (Fig. 12a versus Fig. 12b), modification of the length of the braking period can lead to several potentially fruitful effects.

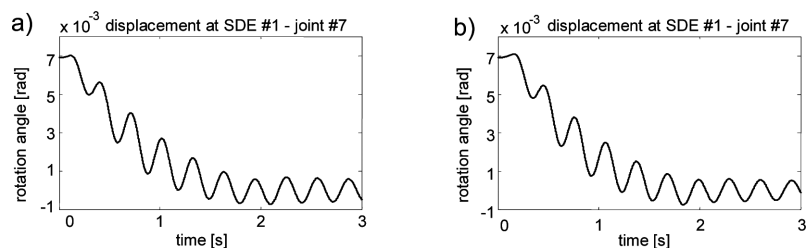


Fig. 13. Displacements at selected *SDEs* of the modelled flexible beam (second direction of bending): 2s braking period (a); 1.9s braking period (b)

Before concluding, let us point out, however, that the introduced sub-periods are not easy to observe in the subsequent characteristics expressing the seventh joint motion (see Fig. 13). To explain it, the focus has to be set on the observed correlative between the direction of the *SDE* joint deformations and the trajectory of motions of the beam particles. Then, the first direction is considered for the deformations (i.e., the sixth joint deformations presented in Fig. 12), this direction is collinear to the tangent direction of the *SDEs* trajectory in the final period of motion. Thus, the tangent components of the beam accelerations are dominant case of this direction. When the second direction is considered (i.e., the seventh joint deformations presented in Fig. 13), the centrifugal effects are dominant (they are collinear to the normal to the *SDEs* trajectory). As a consequence, decelerations originating from the braking torques (i.e., these applied in the robot joints) can heighten the tangent components of the beam accelerations, and according to the considered orientation of the beam (i.e., to the beam orientation in the sub-period *B*), significant influences can be observed in the firsts directions of the *SDEs* deformations, only. The second directions of deformations of the *SDEs* are weekly dependent on the actual values of the braking torques, while they are stronger dependent on the actual velocities of the beam particles.

## 6. Summary and conclusions

In this paper, a combined modelling method is described. The rigid finite elements modelling and the multibody system modelling are joined together, and benefits of the two modelling methods can be used more effectively. To reduce the sizes of the matrices present in the numerical model, a modified rigid finite elements method is used successfully. The lower order relative

deformations are locked, but instead of the additional constraint equations, kinematic chain structures are introduced and the joint coordinates are used in the model, instead of the absolute coordinates typical in the initial, classical model. The homogenous transformations, as well the Denavit-Hartenberg coordinates are omitted in the present models. An alternative multibody modelling is proposed, the latter being based on the chain relations of kinematics, on Newton/Euler dynamic equations of rigid bodies, on kinetostatic principle, and on projections of the joint interactions. The proposed, multibody modelling turns out to be an effective modelling method.

The obtained simulation results show that a significant reduction of the vibration range is possible when length of the braking period is well adjusted to the properties of beam dynamics. The method is especially effective in the tested planar cases, while in the spatial case, deformations in the normal direction (obtained with respect to the beam trajectory) are weakly influenced by the proposed reduction method. In the tangent direction, the method remains effective.

The results have indicated effectiveness of the method when employed for the middle range of beam elasticity, only. For low elasticity, when long vibration periods are observed, the effective lengths of the braking periods become technologically too long. Their practical realisation may be difficult. For the high elasticity cases, precision is crucial in the estimation of the beam actual position, otherwise the possible estimation errors can distort the result expected in the range reduction. Precise estimation of the beam motion is crucial in the reduction method. Nonlinear effects, present in the dynamic equations, must be taken into consideration. It confirms the necessity of applying the sophisticated model, and the necessity of combining the rigid finite elements and multibody modelling in estimation of the beam behaviour.

Manuscript received by Editorial Board, November 27, 2012;  
final version, February 25, 2013.

#### REFERENCES

- [1] Awrejcewicz J., Krysko A.V., Mrozowski J., Saltykova O.A. and Zhigalov M.V.: Analysis of regular and chaotic dynamics of the Euler-Bernoulli beams using finite difference and finite element methods, *Acta Mechanica Sinica*, **27/1**, 36-43, 2011.
- [2] Awrejcewicz J., Krysko A.V., Zhigalov M.V., Saltykova O.A. and Krysko V.A.: Chaotic vibrations in flexible multi-layered Bernoulli-Euler and Timoshenko type beams, *Latin American Journal of Solids and Structures*, **5/4**, 319-363, 2008.
- [3] Lipiński K.: *A Robot Unit Devoted to Carrying a Common, Thin and Long Load*, in: *Multibody Dynamics 2011: ECCOMAS Thematic Conference*, Brussels, Belgium, 4th-7th July 2011, Université catholique de Louvain. - Brussels, 2011.
- [4] Lipiński K.: *Obciążenia długiego, wiotkiego pręta przenoszonego przez układ robotów*, *Modelowanie Inżynierskie*. - Vol. 10, nr 41 (2011).

- [5] Kruszewski J., Gawroński W., Wittbrodt E., Najbar F. and Grabowski S.: *Metoda sztywnych elementów skończonych*, Arkady, (in Polish), Warszawa, 1975.
- [6] Kruszewski J., Sawiak S. and Wittbrodt E.: *Metoda sztywnych elementów skończonych w dynamice konstrukcji*, WNT, (in Polish), Warszawa, 1999.
- [7] Wittbrodt E., Adamiec-Wójcik I. and Wojciech S.: *Dynamics of flexible multibody systems*, Springer, 2006.
- [8] Wojciech S.: *Dynamika płaskich mechanizmów dziwigniowych z uwzględnieniem podatności ogniw oraz tarcia i luzów w węzłach*, Wydawnictwo Politechniki Łódzkiej, rozprawy naukowe nr 66, (in Polish), Łódź, 1984.
- [9] Fiset P., Lipiński K. and Samin J.C.: Symbolic Modelling for the Simulation, Control and Optimisation of Multibody Systems. Advances in Multibody Systems and Mechatronics, Kecskeméthy, A. Et al. (eds.) Institut für Mechanik und Getriebelehre Technische Universität Graz, Graz, (Austria), Septembre 1999, 1999.
- [10] Lipiński K.: Trajectory tracking problem for a redundantly actuated walking robot. *International Journal of Applied Mechanics and Engineering*, **15/3**, 743-753, 2010.
- [11] Lipiński K.: *Układy wieloczłonowe z więzami jednostronnymi w zastosowaniu do modelowania złożonych układów mechanicznych*, Wydawnictwo Politechniki Gdańskiej. Seria Monografie 123, (in Polish), Gdańsk, 2012.
- [12] Samin J.C., Fiset P.: *Symbolic Modeling of Multibody Systems*. Kluwer Academic Publisher, Dordrecht, 2003.
- [13] Lipiński K.: *Sztywne elementy skończone w modelowaniu drgań wirującej belki napędzanej silnikiem prądu stałego zasilanym z prostownika tyrystorowego*, (in Polish), Modelowanie Inżynierskie, **36/5**, 2008.
- [14] Lipiński K., Kneba Z.: *Rigid Finite Element Modeling for Identification of Vibrations in Elastic in Elastic Rod Driven by a DC-motor Supplied from a Thyristor Rectifier*, Solid State Phenomena, **164**, 2010.
- [15] Lipiński K., Wittbrodt E.: *Rigid finite elements and multibody dynamics in modelling of elastic shafts*, in: Multibody Dynamics 2009: An ECCOMAS Thematic Conference, Warsaw, Poland, 29th June - 2nd July 2009. / ed. K. Arczewski, J. Frączek, M. Wojtyra; Warsaw Univ. of Technol., Warsaw, 2009.
- [16] Frączek J., Wojtyra M.: *Kinematyka układów wieloczłonowych, metody obliczeniowe*, WNT, Warszawa, 2008 (in Polish).

#### **Zastosowanie sztywnych elementów skończonych i modelowania wieloczłonowego do estymacji i redukcji drgań pręta**

##### Streszczenie

W pracy przedstawiono zagadnienia dynamiki układu mechanicznego złożonego z robota (manipulatora) oraz przeniesionego, elastycznego pręta. Podczas ruchu, w większości z rozważanych przypadków praktycznych, w pręcie generowane są drgania o znaczących amplitudach. Drgania te są szczególnie dobrze widoczne, gdy analizowany jest krótki okres następujący zaraz po zatrzymaniu robota. By zredukować niekorzystne drgania, zaproponowano algorytm sterujący, bazujący na szacowaniu i modyfikacji czasu hamowania (przy założeniu stałych wartości przyspieszeń/opóźnień występujących w przegubach analizowanego robota). W pracy ograniczono się do prezentacji badań numerycznych. Stosowny model numeryczny uzyskano łącząc zasady modelowania, jak i fizyczne fragmenty układu modelowane za pomocą sztywnych elementów skończonych z fragmentami modelowanymi za pomocą zasad dynamiki układów wieloczłonowych. W przywołanej metodzie sztywnych elementów skończonych, zrezygnowano z wersji klasycznej na rzecz metody zmodyfikowanej. W metodzie tej niektóre (wybrane) kierunki deformacji względnych są blokowane. Prowadzi to do istotnej redukcji rozmiaru wyprowadzanych macierzy, jak i do istotnej redukcji czasu poświęconego na wykonywane operacje numeryczne.